Aorta Centerline Smoothing and Registration Using Variational Models

Luis Alvarez[1*], Daniel Santana-Cedrés[1], Pablo G. Tahoces[2], and José M. Carreira[3]

[1] CTIM, DIS, Universidad de Las Palmas de Gran Canaria, Spain
[2] DEC, Universidad de Santiago de Compostela, Spain
[3] Complejo Hospitalario Universitario de Santiago (CHUS), Spain
lalvarez@ulpgc.es,dsantana@ctim.es
{pablo.tahoces,josemartin.carreira}@usc.es

Abstract. In this work we present an application of variational techniques to the smoothing and registration of aorta centerlines. We assume that a $3D$ segmentation of the aorta lumen and an initial estimation of the aorta centerline are available. The centerline smoothing technique aims to maximize the distance of the centerline to the boundary of the aorta lumen segmentation but keeping the curve smooth. The proposed registration technique computes a rigid transformation by minimizing the squared Euclidean distance between the points of the curves, using landmarks and taking into account that the curves can be of different lengths. We present a variety of experiments on synthetic and real scenarios in order to show the performance of the methods.

Keywords: aorta centerline, 3D curve smoothing, 3D curve registration, variational methods.

1 Introduction

Aorta segmentation and centerline estimation from CT scans is an important issue in the diagnosis of cardiovascular diseases. In this paper, we present an application of variational techniques to the smoothing and registration of aorta centerlines. We will assume that we have previously estimated a segmentation of the aorta lumen, given by a 3D set A, and an initial estimation of the aorta centerline, $\mathcal{C}(s)$, given by a $3D$ curve $\mathcal{C} : [0, |\mathcal{C}|] \to R^3$, where s represents the arc-length parameter and $|\mathcal{C}|$ the length of the curve. As shown in section 2, there are a variety of techniques to obtain the aorta segmentation and centerline.

One of the main motivations of this paper is that usually, the centerline estimation techniques include noise in the location of the aorta centerline points. This noise can produce significant errors in some important aorta measures as the aorta length between 2 given points which is a critical measure in some medical treatments such as aortic stent implantations. To address this problem, we propose a centerline smoothing procedure inspired by the following variational model introduced in [7]:

$$\mathcal{C}_w = \underset{\mathcal{C}:\mathcal{C}(0)=p_0,\mathcal{C}(|\mathcal{C}|)=p_1}{\arg\min} \int_0^{|\mathcal{C}|} P(\mathcal{C}(s))ds + w|\mathcal{C}|, \tag{1}$$

where $P(x)$ is the potential, $|\mathcal{C}|$ is the curve length, and $w \geq 0$ is a parameter to balance both terms. In [7], the authors deal with $2D$ curves. However, in our approach, we extend the formulation to $3D$ curves.

The second topic we address in this paper is the registration of 2 centerlines. This is an important issue for patients follow-up, when different CT-scans are acquired in different periods of times. To facilitate the registration procedure, we take into account that given the way the CT scan is obtained, the point $\mathcal{C}(s_0)$ in the aortic arch with minimum z value (if the scan is performed from head to feet, which it is usually the case) can be used as an aortic landmark.

The main contribution of this paper is the application of variational techniques to aorta centerline smoothing and registration. In the case of smoothing, we use the model proposed in [7] but extended to $3D$ curves, using as potential the signed distance function to the aorta segmentation boundary. We propose a completely new numerical scheme adapted to 3D curves. In the case of aorta registration, we propose to compute the rigid transformation between 2 aorta centerlines using landmarks and minimizing the squared Euclidean distance between the corresponding points of both curves. Futhermore, the energy used allows the registration of curves of different lengths. In fact, the smoothing and the registration of centerlines are related problems and as the experiments carried out in this work show, smoothing the centerlines improves the accuracy of the registration.

The rest of the paper is organized as follows: in section 2, we present some related works. In section 3, we study in details the proposed variational method for aorta centerline smoothing. In section 4, we describe the variational method for centerline registration. In section 5, we show some experiments on synthetic and real centerlines. Finally, in section 6, we present some conclusions.

2 Related Work

Automatic aorta segmentation algorithms from CT scans have been previously developed (see [10] for a survey). For instance, in [13], the authors proposed an iterative method based on building a 2-D region for segmenting the ascending aorta. In [2], a tracking procedure of the aorta centerline is presented. In [12], the authors introduce a method for the automatic estimation of the aorta segmentation and the centerline estimation. In [1], an active contour method for the aorta segmentation is proposed.

In [5] and [11], some energies for curvature penalized minimal path are proposed to regularize $2D$ curves. In [4], the authors propose a minimal path approach for tubular structures segmentation in $2D$ images with applications to retinal vessel segmentation.

Concerning 3D curve registration, the iterative closest point (ICP) (see [3]), is a general purpose method for the registration of 3D curves and surfaces which requires initialization of the expected rigid transform. In [9], the authors introduce a scale-space approach for registration of tree vessel structures.

3 Variational Methods for Aorta Centerline Smoothing

In order to perform the aorta centerline smoothing, we propose an extension to 3D curves of the variational model (1) introduced in [7] for $2D$ curves. We use as potential $P(x)$ the signed distance function $d_{\partial A}(x)$ to the boundary of the aorta segmentation A given by

$$P(x) = d_{\partial A}(x) = \begin{cases} d(x, \partial A) & if\ x \notin A, \\ -d(x, \partial A) & if\ x \in A. \end{cases} \tag{2}$$

Using this potential in (1) we aim to maximize the distance between the centerline and the boundary of the aorta lumen segmentation, but keeping the curve smooth. Thus, the final variational model for the aorta centerline smoothing is given by

$$\mathcal{C}_w = \underset{\mathcal{C}:\mathcal{C}(0)=p_0, \mathcal{C}(|\mathcal{C}|)=p_1}{\arg\min} E_S(\mathcal{C}) \equiv \int_0^{|\mathcal{C}|} d_{\partial A}(\mathcal{C}(s))ds + w|\mathcal{C}|, \tag{3}$$

where the parameter w balances both both energy terms. The larger the value of w, the more regular the curve is expected to be.

Numerical scheme to minimize energy (3)

We propose a basic numerical scheme to minimize energy (3). In practice, the centerline $\mathcal{C}$ is given by a collection of $3D$ points $\{\mathcal{C}_i\}_{i=1,..,N_\mathcal{C}}$, where $\mathcal{C}_1 = p_0$ and $\mathcal{C}_{N_\mathcal{C}} = p_1$. We assume that

$$\begin{aligned} \|\mathcal{C}_i - \mathcal{C}_{i-1}\| &= h \quad \text{for all } i = 2, .., N_\mathcal{C} - 1, \\ \|\mathcal{C}_{N_\mathcal{C}} - \mathcal{C}_{N_\mathcal{C}-1}\| &\leq h, \end{aligned} \tag{4}$$

that is, we use a curve parameterization with constant arc-length h. Usually h depends on the image spacial resolution of the CT scan. Typically, h ranges from 0.5mm to 1mm.

For the left part of energy (3), we consider in each point $\mathcal{C}_i$ a gradient descent type scheme of the form

$$\mathcal{C}_i^{n+1} = \mathcal{C}_i^n - \delta \nabla d_{\partial A}(\mathcal{C}_i^n). \tag{5}$$

To simplify the numerical scheme of the right part of energy (3) we consider the curvature shortening flow described, for instance, in [6]. This flow tends to reduce the length of the curve and can be formulated as follows:

$$\mathcal{C}_i^{n+1} = \mathcal{C}_i^n + \delta k_i^n \mathcal{N}_i^n, \tag{6}$$

where k_i^n represents an approximation to the $2D$ curvature and $\mathcal{N}_i^n$ the unit normal direction in $\mathcal{C}_i^n$ of the curve restricted to the plane given by the points

$\mathcal{C}_{i-1}^n, \mathcal{C}_i^n, \mathcal{C}_{i+1}^n$. By combining both schemes and adding the weight w, we obtain the following minimization scheme for (3)

$$\mathcal{C}_i^{n+1} = \mathcal{C}_i^n - \delta \nabla d_{\partial A}(\mathcal{C}_i^n) + \delta w k_i^n \mathcal{N}_i^n, \tag{7}$$

where $\delta > 0$ represents the discretization step. We point out that, after each iteration, we need to reparameterize $\{\mathcal{C}_i^{n+1}\}$ in order to preserve the constant arc-length condition (4). We compute the unit normal vector $\mathcal{N}_i^n$ as

$$\mathcal{N}_i^n = \begin{cases} \frac{\frac{\mathcal{C}_{i-1}^n + \mathcal{C}_{i+1}^n}{2} - \mathcal{C}_i^n}{\left\| \frac{\mathcal{C}_{i-1}^n + \mathcal{C}_{i+1}^n}{2} - \mathcal{C}_i^n \right\|} & \text{if } \frac{\mathcal{C}_{i-1}^n + \mathcal{C}_{i+1}^n}{2} \neq \mathcal{C}_i^n, \\ \overrightarrow{0} & \text{otherwise,} \end{cases} \tag{8}$$

and the curvature k_i^n is approximated as the quotient between the angle, $\theta_i^n = \angle \mathcal{C}_{i-1}^n \mathcal{C}_i^n \mathcal{C}_{i+1}^n$, of the vectors $\overrightarrow{\mathcal{C}_{i-1}^n \mathcal{C}_i^n}$ and $\overrightarrow{\mathcal{C}_i^n \mathcal{C}_{i+1}^n}$ and the arc-length h, that is

$$k_i^n = \frac{\theta_i^n}{h}. \tag{9}$$

We use as stopping criterion of the iterative scheme (7) the condition

$$\frac{|E_S(\mathcal{C}^n) - E_S(\mathcal{C}^{n-1})|}{|E_S(\mathcal{C}^{n-1})|} < \epsilon, \tag{10}$$

where $E_S(\mathcal{C})$ is the energy defined in (3). $\epsilon > 0$ is a parameter to fix the stopping criterion of the scheme. In the experiments presented in this paper we use $\epsilon = 10^{-8}$.

Scheme (7) is a basic approximation of a minimizer of energy (3) but it is not derived from the Euler-Lagrange equation of (3) due to the choice of the curvature shortening flow introduced in (6). Nevertheless, despite this theoretical limitation, in the experiments we show that scheme (7) behaves as a good minimizer of (3) (see Fig. 3).

Automatic estimation of the discretization step δ.

We can estimate δ automatically using a two-step process: on the one hand, using as potential $P(x)$ the normalized signed distance function, we have that $\|\nabla P(\mathcal{C}_i^n)\| \leq 1$. Therefore, by imposing in the scheme (5) that

$$\delta \leq \frac{h}{2}, \tag{11}$$

we obtain that the point $\mathcal{C}_i^{n+1}$ is closer to $\mathcal{C}_i^n$ than to $\mathcal{C}_{i-1}^n$ and $\mathcal{C}_{i+1}^n$. On the other hand, with respect to the curvature part we impose that

$$\delta w k_i^n \leq \left\| \frac{\mathcal{C}_{i-1}^n + \mathcal{C}_{i+1}^n}{2} - \mathcal{C}_i^n \right\|, \tag{12}$$

which means that the curvature flow never makes the point $\mathcal{C}_i^n$ to move to the other side of the segment $\overline{\mathcal{C}_{i-1}^n \mathcal{C}_{i+1}^n}$. Using a straightforward computation, we obtain that the above condition is equivalent to

$$\delta w \frac{\theta_i^n}{h} \leq h \cos\left(\frac{\pi - \theta_i^n}{2}\right). \tag{13}$$

We observe that the function

$$f(\theta) = \delta w \frac{\theta}{h} - h \cos\left(\frac{\pi - \theta}{2}\right), \tag{14}$$

satisfies that

$$f(\pi) = \delta w \frac{\pi}{h} - h \leq 0 \Leftrightarrow \delta \leq \frac{h^2}{w\pi},$$

and we can easily check that if

$$\delta \leq \frac{h^2}{w\pi}, \tag{15}$$

then $f(\theta) \leq 0$ for any $\theta \in [0, \pi]$ and then (13) is satisfied. Therefore, joining both estimations of δ for each part of the numerical scheme, we can fix automatically δ as

$$\delta = \frac{\min\{\frac{h}{2}, \frac{h^2}{w\pi}\}}{2}. \tag{16}$$

In practice, we experienced that using this choice for δ we obtain a stable numerical evolution of (7).

4 Variational Methods for Aorta Centerline Registration

As mentioned in the introduction, to facilitate the registration procedure, we use the aortic arch point with the minimum value of z, $\mathcal{C}(s_0)$, as an aorta landmark. We can assume that, given two centerlines $\mathcal{C}$ and $\mathcal{C}'$ of the same patient and their corresponding landmarks s_0 and s_0', the corresponding point of $\mathcal{C}(s_0)$ in the other centerline is in a vicinity of $\mathcal{C}'(s_0')$. Notice that one landmark can not correspond exactly with the other one because a modification in the patient position during the CT scan acquisition can produce that both landmarks do not match exactly.

Given 2 corresponding positions s_0 and s' in both centerlines, that is $\mathcal{C}(s_0)$ corresponds to $\mathcal{C}'(s')$, we obtain the $3D$ rigid transformation (given by a 3×3 rotation matrix and a $3D$ translation vector t) which transforms $\mathcal{C}'$ into $\mathcal{C}$ by minimizing the following energy

$$E(s_0, s', R, t) = \frac{\int_{\max\{-s_0, -s'\}}^{\min\{-s_0+|\mathcal{C}|, -s'+|\mathcal{C}'|\}} ||(\mathcal{C}(s+s_0) - (R \cdot \mathcal{C}'(s+s') + t)\,||_2^2 ds}{\min\{-s_0+|\mathcal{C}|, -s'+|\mathcal{C}'|\} - \max\{-s_0, -s'\}}. \tag{17}$$

As showed below, for a fixed value of s_0, s', the above minimization problem has a close-form solution. The energy (17) takes into account that the length of both centerlines can be different. Indeed, for instance, according to the way the CT acquisition is performed the size of the aortic centerline in the abdominal area can be different. Finally, we compute the best rigid transformation between both centerlines as

$$(R,t) = \underset{s' \in [s'_0 - r, s'_0 + r]}{\arg\min} E(s_0, s', R, t), \tag{18}$$

where $r \geq 0$ is a parameter which determines the vicinity of the landmark $\mathcal{C}'(s'_0)$ used to look for the point $\mathcal{C}'(s')$ corresponding to the landmark $\mathcal{C}(s_0)$.

Close form solution of the minimization problem (17)

We observe that, in practice, if s_0 and s' are fixed and the curves are discretized, then the minimization problem (18) is equivalent to minimize the energy

$$\tilde{E}(R,t) = \sum_i ||(\mathcal{C}_{i+i_0} - \left(R \cdot \mathcal{C}'_{i+i'} + t\right)||_2^2,$$

for a certain range of i values. In [8], it is showed that this minimization problem has a close-form solution based on a quaternion representation of the rotation matrix (see [8] for more details). We point out that the rigid transformation obtained with the proposed method can be used as an initial guess for iterative methods like ICP (see [3]).

5 Experimental Setup

To verify the accuracy of the proposed method for smoothing the centerline of the aorta, we build the aorta synthetic phantom illustrated in Fig. 1. This centerline is used as an approximation of a real one. The discretized arc-length h (see (4)) is taken equal to 1. Using this centerline we build an aorta segmentation by drawing spheres centered in the aorta centerline points. The radii of the spheres is taken in the range of values expected along real centerlines. To study the convergence of the numerical scheme (7), we add some noise to the position of the original centerline points $\{\mathcal{C}_i\}_{i=1,..,N_{\mathcal{C}}}$ in the following way

$$\mathcal{C}_i^0 = \mathcal{C}_i + (6 + \mathcal{U}(-1,1), 6 + \mathcal{U}(-1,1), 6 + \mathcal{U}(-1,1))^T, \tag{19}$$

where $\mathcal{U}(-1,1)$ follows the uniform probability distribution in the interval $[-1,1]$. We use $\mathcal{C}^0$ as the initial guess for the scheme (7). To evaluate the robustness and convergence of the algorithm $\mathcal{C}^0$ is chosen quite far from the ground truth. We denote by $\mathcal{C}_w^\infty$ the asymptotic state of the scheme (7) accordingly to the parameter w and the stopping criterion (10). In this case the original centerline $\mathcal{C}$ represents the ground-truth and the curve $\mathcal{C}_w^\infty$ represents an approximation of $\mathcal{C}$. In Fig. 1 we show the curves $\mathcal{C}$, $\mathcal{C}^0$ and $\mathcal{C}_w^\infty$ for $w = 0, 1, 10, 50$. We observe that for the values $w = 0, 1, 10$, the smoothed curve $\mathcal{C}_w^\infty$ is close to the original centerline $\mathcal{C}$. However, for $w = 50$, the smoothing effect is too strong and $\mathcal{C}_{50}^\infty$ is

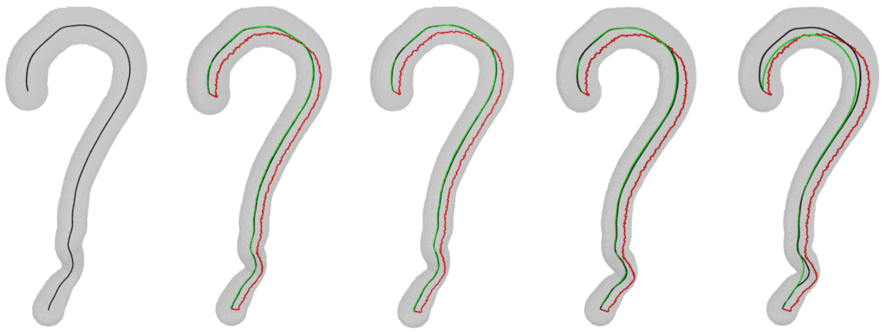

Fig. 1. From left to right we show the original synthetic centerline $\mathcal{C}$, in black, and the segmentation of the aorta phantom in grey (first image). Next we show the curves $\mathcal{C}$ (black), $\mathcal{C}^0$ (red), and $\mathcal{C}_w^\infty$ (green) for $w = 0, 1, 10, 50$.

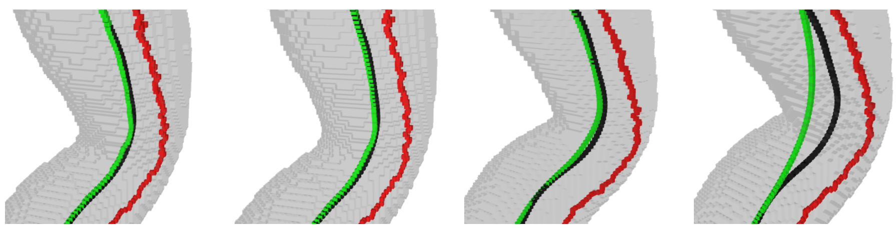

Fig. 2. From left to right we show a zoom of the abdominal area of the aorta phantom where we can see the original centerline, $\mathcal{C}$ (black), the segmentation of the aorta phantom (grey) and the curves $\mathcal{C}^0$ (red) and $\mathcal{C}_w^\infty$ (green) for $w = 0, 1, 10, 50$.

quite far from $\mathcal{C}$. In Fig. 2 we show a zoom of the same curves in the abdominal area, where we can appreciate the influence of the smoothing parameter w.

To measure the quality of the approximation in a quantitative way, we use, as approximation error, the following distance between the ground-truth $\mathcal{C}$ and the approximation $\mathcal{C}^n$:

$$d(\mathcal{C}, \mathcal{C}^n) = \sqrt{\frac{1}{2N_{\mathcal{C}}} \sum_{i=1}^{N_{\mathcal{C}}} d^2(\mathcal{C}_i, \mathcal{C}^n) + \frac{1}{2N_{\mathcal{C}^n}} \sum_{i=1}^{N_{\mathcal{C}^n}} d^2(\mathcal{C}_i^n, \mathcal{C})}, \tag{20}$$

where, for a given $3D$ point p and a curve $\mathcal{C}$, $d(p, \mathcal{C})$ is the Euclidean distance of p to the curve $\mathcal{C}$. In table 1 we present some quantitative results about the number of iterations using the stopping criterion (10), the length $|\mathcal{C}_w^\infty|$, the energy $E_S(\mathcal{C}_w^\infty)$ defined in (3) and the error $d(\mathcal{C}, \mathcal{C}_w^\infty)$ defined by (20). We observe that the error $d(\mathcal{C}, \mathcal{C}_w^\infty)$ is similar for $w = 0$ and $w = 1$. However, there is an important difference with respect to the centerline length. The length of the original curve $\mathcal{C}$ is 457mm, whereas the length of $\mathcal{C}_0^\infty$ is much larger (464.86mm). The reason for this length discrepancy is that if we remove the smoothing term, the obtained

3D curve tends to zigzag, which produces an artificial increase of the centerline length. The length of $\mathcal{C}_1^\infty$ (458.05mm) is much closer to the original one.

Table 1. Quantitative results obtained for the phantom centerline $\mathcal{C}_w^\infty$ for $w = 0, 1, 10, 50$.

w	N. Iterations(10)	Final Length (mm)	Final Energy $E_S(\mathcal{C}_w^\infty)$ (3)	Final Error (mm) (20)
0	352	464.86	−6728.28	0.670 057
1	267	458.05	−6184.34	0.676 328
10	1721	453.39	−2031.11	0.733 271
50	4556	428.74	16 128.73	4.094 052

In Fig. 3, 4 and 5 we show, for different values of w, the evolution of the length of $\mathcal{C}^n$, the energy $E_S(\mathcal{C}^n)$ and the error $d(\mathcal{C}, \mathcal{C}^n)$ for the first 1000 iterations of scheme (7). We observe a nice convergence behavior of $E_S(\mathcal{C}^n)$. As expected, the evolution of the length of $\mathcal{C}^n$ is strongly influenced by the value of w, and if the smoothing parameter w is too high, $\mathcal{C}^n$ does not converge towards $\mathcal{C}$.

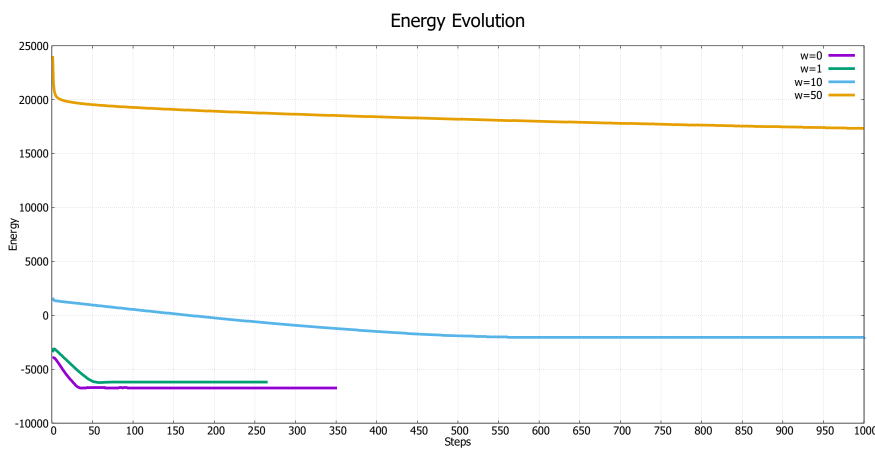

Fig. 3. Evolution of $E_S(\mathcal{C}^n)$ for the phantom centerline with different values of w.

In Fig. 6 we illustrate the results of the proposed method for centerline smoothing using a real CT scan. We can observe in the figure the smoothing effect introduced by the curve regularization.

Next, we present some experiments to show the accuracy of the proposed 3D curve registration technique. We use 2 CT scans of the same patient provided to us by the Department of Radiology of the University Hospital of Santiago de Compostela, Spain. In Fig. 7, we compare the centerlines and segmentations obtained from both CT scans before and after registration using the original

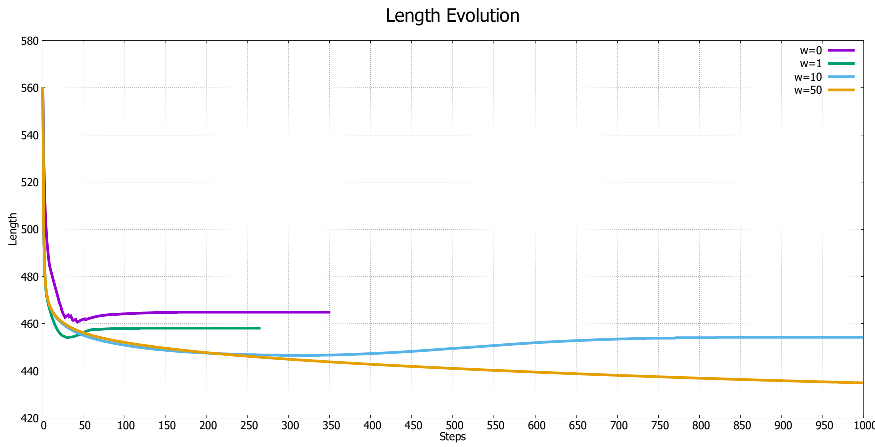

Fig. 4. Evolution of $|\mathcal{C}^n|$ for the phantom centerline with different values of w.

centerlines. The average squared distance error obtained in the centerline registration given by (18) is 7.54 mm. We also compute the distance between the boundaries of the segmentations. We use a colormap to illustrate such distance (blue means distance 0 and red distance 3.5 (in mm)).

In Fig. 8, we show the results of the same experiment but the centerlines have been previously smoothed. In this case, the average squared distance error obtained in (18) is 1.38 mm, which is much smaller than the one previously obtained without smoothing the centerlines. In particular, it means that by smoothing the centerlines we improve the accuracy of the registration procedure. This behaviour is expected due to the noise present in the original centerlines. This noise introduces disturbances in the centerline parameterizations that can produce significant errors in the registration procedure. By smoothing the centerlines, we strongly reduce these errors, achieving a greater precision in the calculation of the distance between any two points of the centerline of the aorta. This result could be of great interest for the development of medical applications, where the precise measurement of distances is necessary for the diagnosis of diseases and follow-up of patients.

6 Conclusions

In this paper we have presented an application of variational models to the problem of aorta centerline smoothing and registration which are both relevant issues in medical imaging. For centerline smoothing we use an extension to $3D$ curves of a well-known variational model introduced in [7] for $2D$ curves and we propose a completely new numerical scheme. The proposed method for centerline registration is based on curve parameterization and the use of landmarks, providing close-form solutions for the estimation of the rigid transformation, even in the

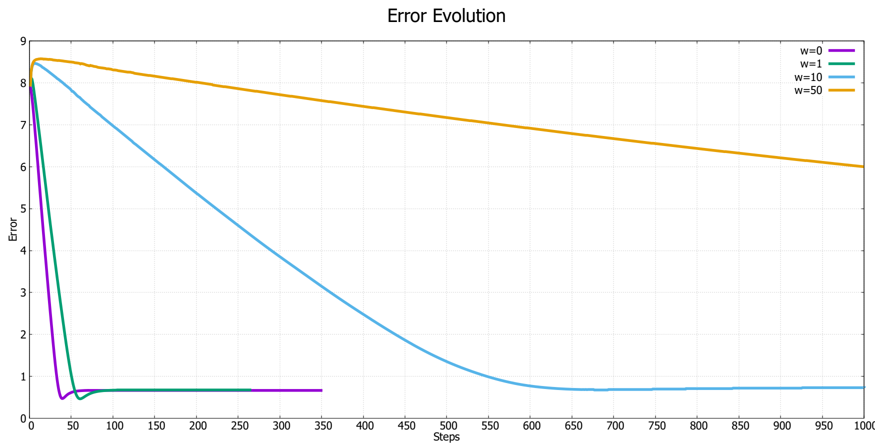

Fig. 5. Evolution of $d(\mathcal{C}, \mathcal{C}^n)$ for the phantom centerline with different values of w.

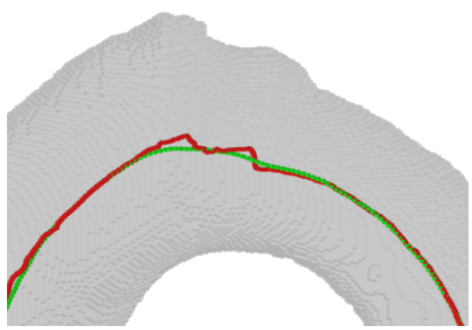

Fig. 6. We present a zoom in the aortic arch of one of the real aortas presented in Fig. 7. We show the segmentation (grey), the original centerline (red) and the centerline smoothed with the proposed method with $w = 1$ (green).

case of curves of different lengths. The experiments performed on synthetic and real centerlines for both methods provide promising results. In particular, we have managed to improve the accuracy of the registration technique by smoothing the centerlines.

Acknowledgement
This research has partially been supported by the MINECO projects references TIN2016-76373-P (AEI/FEDER, UE) and MTM2016-75339-P (AEI/FEDER, UE) (Ministerio de Economía y Competitividad, Spain).

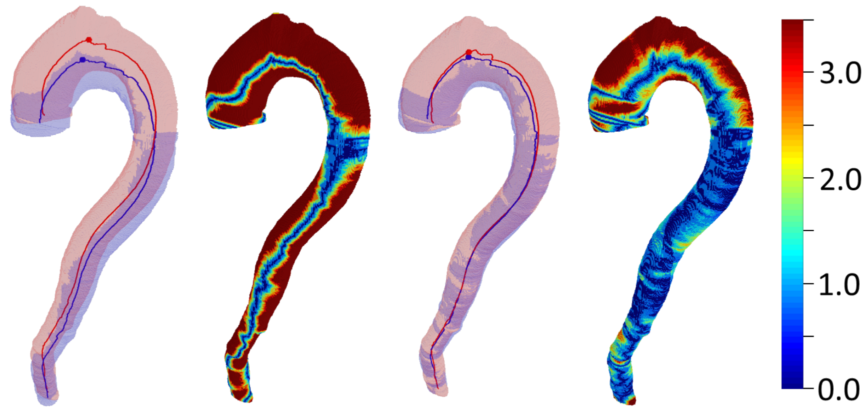

Fig. 7. We compare the centerlines and segmentations obtained from 2 CT scans of the same patient before and after registration. The landmarks used are marked with a sphere. We use the original centerlines and the radius r used in (18) to look in a vicinity of the landmark is $r = 25$. We use a colormap to illustrate the distance between the boundary of both segmentations (before and after registration).

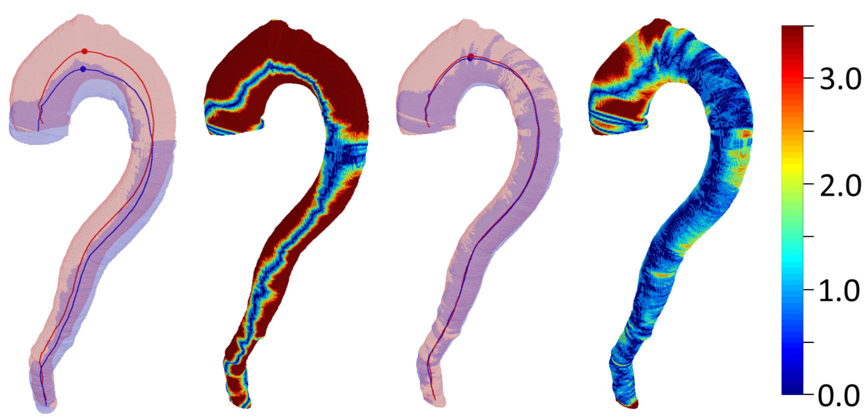

Fig. 8. We perform the same comparison that in Fig. 7 but in this case the centerlines have been previously smoothed with $w = 1$.

References

1. Alemán-Flores, M., Santana-Cedrés, D., Alvarez, L., Trujillo, A., Gómez, L., Tahoces, P.G., Carreira, J.M.: Segmentation of the Aorta Using Active Contours with Histogram-Based Descriptors. In: MICCAI Workshop: Intravascular Imaging and Computer Assisted Stenting and Large-Scale Annotation of Biomedical Data and Expert Label Synthesis. pp. 28–35. Springer International Publishing (2018)
2. Alvarez, L., Trujillo, A., Cuenca, C., González, E., Esclarín, J., Gomez, L., Mazorra, L., Alemán-Flores, M., Tahoces, P.G., Carreira, J.M.: Tracking the Aortic Lumen Geometry by Optimizing the 3D Orientation of Its Cross-sections. In: Medical Image Computing and Computer-Assisted Intervention MICCAI 2017. pp. 174–181. Springer International Publishing, Cham (2017)
3. Besl, P.J., McKay, N.D.: A method for registration of 3-D shapes. IEEE Transactions on Pattern Analysis and Machine Intelligence 14(2), 239–256 (1992)
4. Chen, D., Zhang, J., Cohen, L.D.: Minimal Paths for Tubular Structure Segmentation With Coherence Penalty and Adaptive Anisotropy. IEEE Transactions on Image Processing 28(3), 1271–1284 (March 2019)
5. Chen, D., Mirebeau, J.M., Cohen, L.D.: Global Minimum for Curvature Penalized Minimal Path Method. In: Proceedings of the British Machine Vision Conference (BMVC). pp. 86.1–86.12. BMVA Press (September 2015)
6. Chou, K.S., Zhu, X.P.: The Curve Shortening Problem. Chapman and Hall/CRC (2001)
7. Cohen, L.D., Kimmel, R.: Global Minimum for Active Contour Models: A Minimal Path Approach. International Journal of Computer Vision 24(1), 57–78 (Aug 1997)
8. Faugeras, O.D., Hebert, M.: The Representation, Recognition, and Locating of 3-D Objects. Int. J. Rob. Res. 5(3), 27–52 (Sep 1986)
9. Heldmann, S., Papenberg, N.: A Scale-Space Approach for Image Registration of Vessel Structures. In: Bildverarbeitung für die Medizin (2009)
10. Lesage, D., Angelini, E.D., Bloch, I., Funka-Lea, G.: A review of 3D vessel lumen segmentation techniques: Models, features and extraction schemes. Medical Image Analysis 13(6), 819 – 845 (2009), includes Special Section on Computational Biomechanics for Medicine
11. Mirebeau, J.M.: Fast-Marching Methods for Curvature Penalized Shortest Paths. Journal of Mathematical Imaging and Vision 60(6), 784–815 (Jul 2018)
12. Tahoces, P.G., Alvarez, L., González, E., Cuenca, C., Trujillo, A., Santana-Cedrés, D., Esclarín, J., Gomez, L., Mazorra, L., Alemán-Flores, M., Carreira, J.M.: Automatic estimation of the aortic lumen geometry by ellipse tracking. International Journal of Computer Assisted Radiology and Surgery 14(2), 345–355 (Feb 2019)
13. Wang, S., Fu, L., Yue, Y., Kang, Y., Liu, J.: Fast and Automatic Segmentation of Ascending Aorta in MSCT Volume Data. In: 2009 2nd International Congress on Image and Signal Processing. pp. 1–5 (Oct 2009)